Semi-automated method for the determination of the all-optical monitoring strategy of complex thin-film filters

M Vignaux, F. Lemarchand, T. Begou, C. Grezes-Besset, Julien Lumeau

Research Article | Vol. 27, No. 9 | 29 Apr 2019 | OPTICS EXPRESS 12373
Optics EXPRESS

Semi-automated method for the determination of the all-optical monitoring strategy of complex thin-film filters

M. VIGNAUX,[1,2] F. LEMARCHAND,[1] T. BEGOU[1], C. GREZES-BESSET,[2] AND J. LUMEAU[1,*]

[1]*Aix-Marseille Univ, CNRS, Centrale Marseille, Institut Fresnel, Marseille, France*
[2]*CILAS Etablissement de Marseille, 600 avenue de la Roche Fourcade, Pole ALPHA Sud – ZI Saint Mitre, 13400 Aubagne, France*
**julien.lumeau@fresnel.fr*

Abstract: One of the critical steps in the fabrication of complex optical interference filters is the precise control of the thickness of the layers during the fabrication process. However, the definition of the optimal optical monitoring strategy remains a challenge as it relies on user experience and there is no reliable automatic determination of this strategy. Here, we propose a semi-automated method that allows the determination of the optimal strategy. It is based on the combination of trinary mappings to select spectral regions that are compatible with optical monitoring and the use of the reflected phase error at a single wavelength versus optical monitoring wavelength. We show how this procedure can be used for the determination of either a single optical monitoring wavelength or a multi-wavelength procedure of a complex filter and confirm these theoretical results with an experimental demonstration.

1. Introduction

Optical interference filters offer a very broad range of optical functions for the control of the spectral properties of light. With the last 15-year improvement of both the design techniques and the manufacturing systems, the complexity of filters has dramatically increased [1]. In particular, the combination of stable deposition processes (e.g. sputtering technique) and in situ optical monitoring has allowed fabrication of high performances filters that can be composed with several hundreds of layers [2,3]. While the filters structure used to show some periodicity due to the use of common formulae based on quarter wave layers, the filters that now need to be deposited are no longer periodic and can exhibit a very broad range of thicknesses ranging from a few nanometers to a few hundreds of nanometers for filters in visible and near-IR range. The use of optical criteria such as turning point monitoring (TPM, determination of the moment the derivative of the optical monitoring signals cancels) with easily determined monitoring wavelength is now less and less used and Level-cut (LC, determination of pre-defined optical monitoring signal levels) or a more advanced method such as optical monitoring by swing (or Percentage Of Extremum Monitoring (POEM)) are generally preferred [4,5]. However, while such techniques can accurately determine the moment a deposition has to be stopped, the accuracy highly depends on the selected optical monitoring wavelength. The choice of the optimal optical monitoring wavelength is therefore a critical step that will directly affect the final performances of the filter. Indeed, with some classical [3,6] or very complex filters [7], the error can quickly diverge and result in large discrepancies if the optical monitoring wavelengths are not properly selected.

In this paper, we provide a thorough description of the combination of three methods that can be implemented in order to define an optimal strategy for optical monitoring of optical interference filters. These methods include:

#359780 https://doi.org/10.1364/OE.27.012383
© 2019 Received 7 Feb 2019; revised 11 Mar 2019; accepted 12 Mar 2019; published 17 Apr 2019

Optics EXPRESS

- **Virtual deposition process** (VDP). While such an approach is well-known in the thin film community [8,9], we have developed a custom software that we have then adapted to the specific needs of the developed procedures.
- **φ_{RMSD} (and $\Sigma\varphi_{RMSD}$) or PhaseEval Method**. This quantity is defined as the root mean square deviation of the reflected phase of a multilayer stack (or the cumulative phase error when stack is being built) and is used to estimate, using single wavelength value, the compatibility of a specific optical monitoring wavelength with optical monitoring by swing. φ_{RMSD} is defined as:

$$\varphi_{RMSD} = \sqrt{\frac{\sum_{i=1}^{Npr}\left(\varphi(i)-\varphi_{th}\right)^2}{Npr}}. \quad (1)$$

and $\Sigma\varphi_{RMSD}(N)$ is defined as the sum of the φ_{RMSD} after depositing N layers and represents the cumulative phase average errors after depositing N layers:

$$\sum\varphi_{RMSD}(N) = \sum_{i=0}^{N}\varphi_{RMSD}(i). \quad (2)$$

where φ_{th} is the theoretical reflection phase of the filter at the end of a layer, $\varphi(i)$ the phase of the i^{th} simulated filter, and Npr = 100, the number of predictions. A thorough description of the methods applied to various kinds of bandpass filters can be found [10].

- **Trinary mappings**. These graphs allow to define some paths that are compatible with a given optical monitoring technique (LC, LC by swing and TPM) and rely on some predefined criteria such as the distance to the next extremum, the signal modulation amplitude… A thorough description of the method applied to various kinds of filters can be found in [11].

2. Description of the problem

To perform this study, we have considered a filter with a complex arbitrary profile (in reflection) that matches the inverse of the intensity spectral distribution of a white light source and that can therefore be used in order to equalize the intensity spectral distribution. The advantage of such a component is that the spectral profile cannot be obtained with standard stack formula and the formula also does not show any periodicity. The design of such a filter was performed using Optilayer software [12,13]. Figure 1 shows the expected spectral profile in reflection of the filter and Table 1 provides the associated formula. This filter is composed with 48 layers of alternated low (SiO_2) and high (Nb_2O_5) refractive index materials with thicknesses ranging from 11.6 to 228 nm, without any periodicity or specific structure. Thus, it is expected that the determination of the optimal monitoring procedure is not as straightforward as in the case of a quarter wave structure and that several monitoring wavelengths could be required. In order to find a strategy, the classical approach generally consists in using either the experience of the scientist in charge of the fabrication or to use Optilayer dedicated module [13]. An example of two strategies as determined by Optilayer software are presented hereafter. Indeed, the monitoring strategy takes into account many criteria with ability to weight different requirements. It is based on an exhaustive search approach on several different wavelengths. Considering the complexity and the number of layers (48), we fixed the number of monitoring wavelengths to 3 or 5. A defect function is defined, taking into account 3 criteria. The first one is the final swing value, determined as the ratio of the difference between the trigger-point signal value and maximum of the signal to the signal amplitude. Lower and upper thresholds are fixed to 30% and 70%. Then, a penalty is applied if the amplitude of the signal in the considered layer is below 4%. And finally, the

Optics EXPRESS

distance from the Trigger Point to the next Turning Point should be higher than 2% to ensure an accurate monitoring. The determined strategies are:

$$[1-7]@439\,nm \rightarrow [8-19]@695\,nm \rightarrow [20-48]@987\,nm$$
$$and \qquad (3)$$
$$[1-7]@439\,nm \rightarrow [8-18]@693\,nm \rightarrow [19-22]@563\,nm$$
$$\rightarrow [23-40]@532\,nm \rightarrow [41-48]@630\,nm.$$

One of the main drawbacks of these techniques relies on the fact that while a possible strategy can be found, it is hard to define if selected strategy is optimal. In this paper, we present a method combining virtual deposition process, PhaseEval method and trinary mappings in order to determine all-optical monitoring strategies for this complex filter.

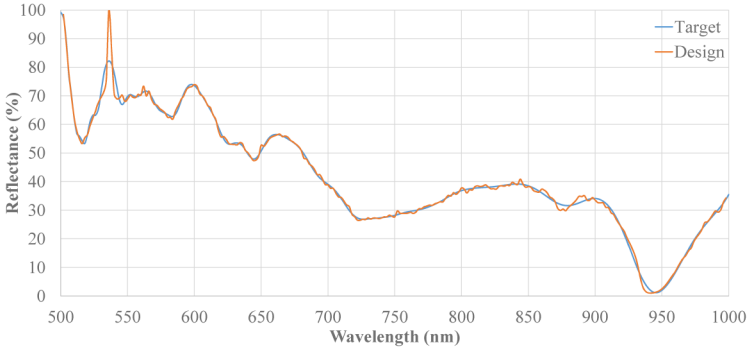

Fig. 1. Spectral dependence of the reflectance of the intensity equalizing filter. In blue the target profile, in red the theoretical profile of the designed filter.

Table 1. Thickness of the layers of the designed equalizing filter (in nanometer).

#	1	2	3	4	5	6	7	8
Material	H	L	H	L	H	L	H	L
Thickness	11.6	64.1	165.7	228.1	156.8	215.8	147.7	228.0
#	**9**	**10**	**11**	**12**	**13**	**14**	**15**	**16**
Material	H	L	H	L	H	L	H	L
Thickness	170.1	208.7	157.6	353.1	145.8	95.3	27.9	85.6
#	**17**	**18**	**19**	**20**	**21**	**22**	**23**	**24**
Material	H	L	H	L	H	L	H	L
Thickness	46.4	231.1	195.8	101.2	117.0	80.8	24.2	74.6
#	**25**	**26**	**27**	**28**	**29**	**30**	**31**	**32**
Material	H	L	H	L	H	L	H	L
Thickness	90.5	79.6	45.8	56.9	150.1	83.3	34.0	57.9
#	**33**	**34**	**35**	**36**	**37**	**38**	**39**	**40**
Material	H	L	H	L	H	L	H	L
Thickness	63.8	68.7	28.5	70.0	181.0	66.4	26.0	82.6
#	**41**	**42**	**43**	**44**	**45**	**46**	**47**	**48**
Material	H	L	H	L	H	L	H	L
Thickness	66.8	46.8	38.2	87.0	40.8	37.7	64.0	139.8

Optics EXPRESS

3. Analysis of the possible paths for optical monitoring

3.1. Trinary mapping analysis

The first step in the determination of all-optical monitoring strategies of such a filter is the generation of the trinary mapping using the procedure described in [11]. We plotted in Fig. 2, the trinary mapping of the whole 48 layers of the filter when optical monitoring is changed from 450 to 1000 nm with a 1 nm step. We limited our analysis to this spectral range as the noise level of our optical monitoring system (Bühler OMS 5000 installed on a Bühler HELIOS machine) significantly increases below 450 nm. Moreover, above 1000 nm, no additional potential path could be revealed. The same color code as the one described in [11] was implemented in this work:

- Grey areas represent spectral ranges where the optical monitoring signal of these given layers is, a priori, not compatible with LC by swing,
- Blue areas are spectral ranges where layers can be monitored using LC by swing,
- Green area are spectral ranges where layers can be monitored using LC by swing and optical monitoring signal crosses two extrema. These layers are considered as optimal layers to start with a new optical monitoring wavelength as LC by swing will self-calibrate the signal and partially compensate for potential fabrication errors.

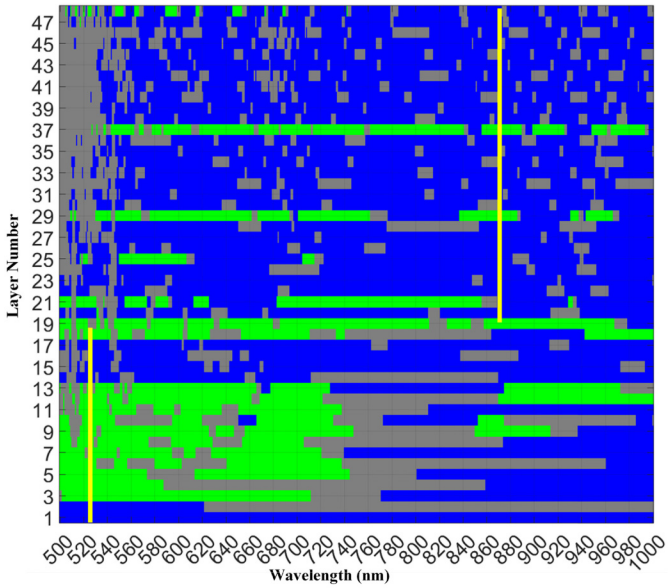

Fig. 2. Trinary mapping of the equalizing filter. Yellow path represent the wavelengths used for a two-wavelength monitoring strategy.

Direct analysis of such a complex mapping can appear quite complicated if not impossible, but it contains a large amount of information. For example:

- Due to the low thickness of the first layers, optical monitoring of the first part of the stack should be performed in the short wavelength range below 740 nm. In addition, the second layer is not compatible with LC by swing for wavelength above 590 nm as the trigger point approaches a turning point for longer wavelengths.
- The largest number of layers that can be optically monitored with one single wavelength is 18 if 524 ± 1 nm is used.

Optics EXPRESS

- Further optical monitoring of the layer thickness requires changing the monitoring wavelength and using a longer wavelength. Accurate analysis of the trinary mapping can show that the optical monitoring of the remaining part of the stack can then be performed with a single wavelength, i.e. 871 ± 1 nm. In conclusion, optimal all-optical monitoring procedure requires using a minimum of 2 different wavelengths shown in yellow in Fig. 2: 524 nm for layers 1 to 18 and 871 nm for layers 19 to 48.
- Finally, one can see that there are a few thick layers, e.g. layers 3 to 13, 18, 19, 25, 29 and 37 which appear in green in the trinary mapping, showing that the associated optical monitoring signal will cross two extrema during the deposition of these layers. These layers will therefore be reliable layers for changing the monitoring wavelength.

3.2. Description of the procedure

In order to determine an all-optical monitoring strategy, the procedure that we have implemented in this work is the following:

1. Using the trinary mapping in Fig. 2, we determined the potential paths that are trigger point monitoring-compatible starting at layer 1.
2. We then analyzed among these potential paths what are the paths that allow all-optical monitoring of the largest number of layers.
3. In order to select part of these possible paths we forced the strategy to change the monitoring wavelength only at a layer N which trinary mapping is green, i.e. a layer that appears as optimal for starting optical monitoring with a new wavelength.
4. For these potential wavelengths, we implemented the PhaseEval method and selected the wavelength that allowed securing the lowest value of φ_{RMSD} and $\Sigma\varphi_{RMSD}$ for each layer and fixed this wavelength as optimal wavelength for monitoring layers 1 to N-1.
5. We then analyzed the potential wavelengths for layer N and after, that are compatible with LC by swing and which optical monitoring signal crosses two extrema (green rectangles) and apply the procedure that is described in points 1 to 5 for the remaining part of the stack.

Figure 3 illustrates the principle of the proposed method.

Optics EXPRESS

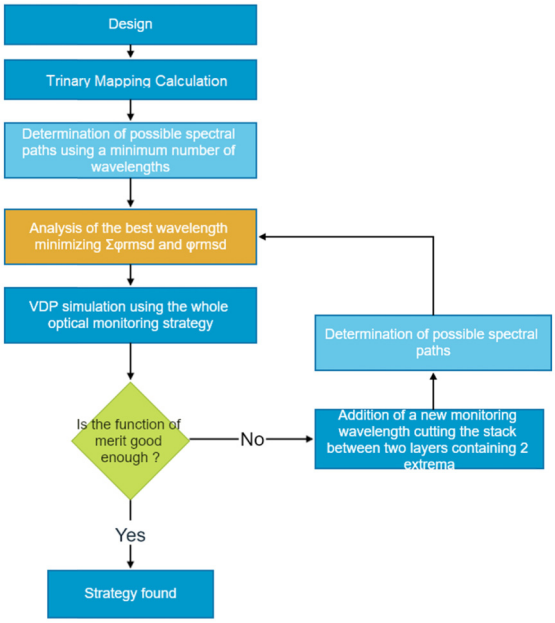

Fig. 3. Decision tree used to optimize the optical monitoring strategy of a thin film optical component.

3.3. Determination of the wavelength to select for PhaseEval method implementation

In [10], the PhaseEval method was shown to provide useful information for the determination of an efficient all-optical monitoring procedure especially for bandpass filters. φ_{RMSD} is calculated at a single wavelength that needs to be determined. While the central wavelength of the bandpass appeared as legitimate for bandpass filters in order to secure perfect centering of the filter, the choice of the φ_{RMSD} calculation wavelength is not as straightforward when it comes to such a complex filter. It is important to remind that the reason for using phase deviation information instead of intensity deviation information is the fact that it is intended that the phase change due to layer thickness errors are less random that the associated intensity fluctuations and therefore easier to quantify with a single wavelength evaluation. Phase error deviation also allows for compensation mechanisms which wouldn't be possible if we only search for the lowest possible thickness per layer. However, such a conclusion is valid only in regions where phase varies linearly and far from those that present a sign change of the slope. To evaluate the optimal wavelengths for PhasEval method implementation (and thus φ_{RMSD} calculation), we calculated the evolution of the sign of the phase changes for each layer when its thickness is increased by 1 nm for every considered optical monitoring wavelength (Fig. 4). Yellow squares represent positive phase change while blue squares represent negative phase change. One can see that depending on the layer number, a change of the sign of the phase happens at different monitoring wavelengths (transition from yellow to blue or vice-versa along one line). Moreover, the number of sign change varies depending on the number of deposited layers. There are several spectral ranges that appear as optimal for selecting the wavelengths (e.g. ~895, 700 nm…), and some spectral regions that should be avoided as they show sharp changes of the sign of the phase change, e.g. some narrow bands in the [500-600] or [920-970] nm spectral range for example.

Optics EXPRESS

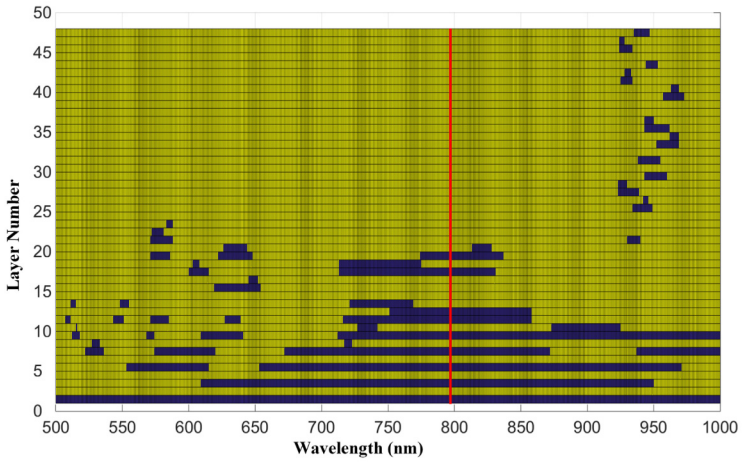

Fig. 4. Evolution of the sign of the phase change for each layer when the thickness of one layer is increased by 1 nm for every considered optical monitoring wavelength. Yellow squares represent positive phase change while blue squares represent negative phase change. The red line represents the selected wavelength: 795 nm.

To implement the PhaseEval method, we selected, in this paper, 795 nm (shown as a red line in Fig. 4) as the reference wavelength as it seems to be a wavelength where the sign of the phase change for each layer appears constant and pretty uniform when the thickness of one layer is increased by 1 nm. Also, this wavelength lies within the central part of the spectral region where the performances of the filter are specified [500-1000] nm. Therefore, one can expect that a stable phase value at 795 nm, i.e. small values of φ_{RMSD} and $\Sigma\varphi_{RMSD}$, will allow securing stable broadband spectral performances in intensity. Moreover, it is worth mentioning that other wavelengths were implemented for the PhaseEval method such as 470, 510 and 640 nm. As expected, depending on the tested layers, 510 nm did not provide the exact same information as 470 or 795 nm. However, very similar trends could be extracted for all wavelengths, confirming that PhaseEval method at a single wavelength is an interesting technique for evaluating the overall broadband spectral performances of an optical filter.

3.4. Determination of an all optical monitoring procedure of an equalizing filter

We implemented the trinary mapping and the PhaseEval method to determine various optical monitoring strategies using different numbers of optical monitoring wavelengths and extract the best of them.

3.4.1. Two-wavelength strategy

Let us consider the trinary mapping in Fig. 2. We have already seen that it is possible to optically monitor the whole stack with a minimum of 2 wavelengths. Let us analyze the performance of such a strategy. At first, let us focus on the spectral region that appears as compatible with LC by swing for the first layers, i.e. [450-600] nm and let us plot, for each wavelength, the maximum number of layers that can be optically monitored with a single wavelength (Fig. 5).

Optics EXPRESS

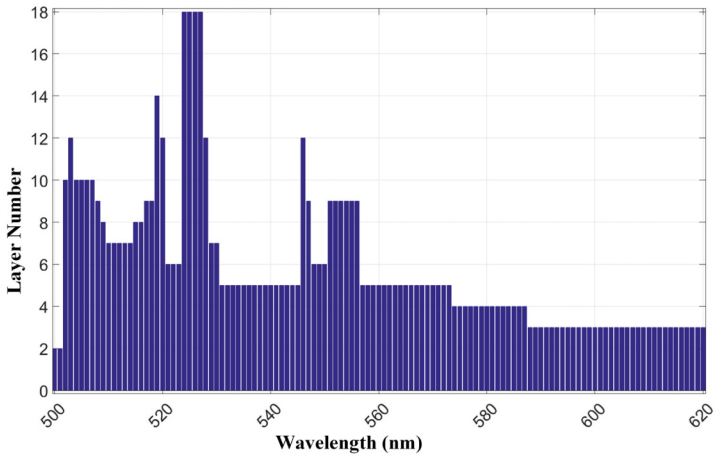

Fig. 5. Maximum number of layers that can be optically monitored with a single wavelength in the [500-620] nm spectral region.

One can see that the maximum number of layers that can be optically monitored is equal to 18. The strategy that we propose to implement here relies in finding the wavelength that allows optical monitoring up to a layer N as large as possible but the chosen layer must allow for the new monitoring wavelength to begin at a double-extremum layer which trinary mapping is green, i.e. a layer that appears as optimal for starting optical monitoring with a new wavelength. These so-called green layers can be found at layers 3 to 13 and then 18 and 19 (Fig. 2). One can see that the range of wavelengths that combines both criteria are 524, 525, 526 and 527 nm. They allow all-optical monitoring of layers 1 to 18 and optical monitoring wavelength is then changed at layer 19.

In order to determine which of these wavelengths appears to be the best, we then implemented the PhaseEval method @795 nm when depositing the 18 first layers (Fig. 6). One can see that the value of $\Sigma\varphi_{RMSD}$ is pretty uniform. There are some fluctuations in this range, but those one are pretty small and might be related to the statistical nature of the analysis. We however opted for the wavelength that shows the lowest overall value of $\Sigma\varphi_{RMSD}$, i.e. 524 nm. One can also see that main phase errors appear at layer 14 and changing before this layer would be a possible option to try to improve the optical monitoring strategy, but might require using a larger number of wavelengths.

Optics EXPRESS

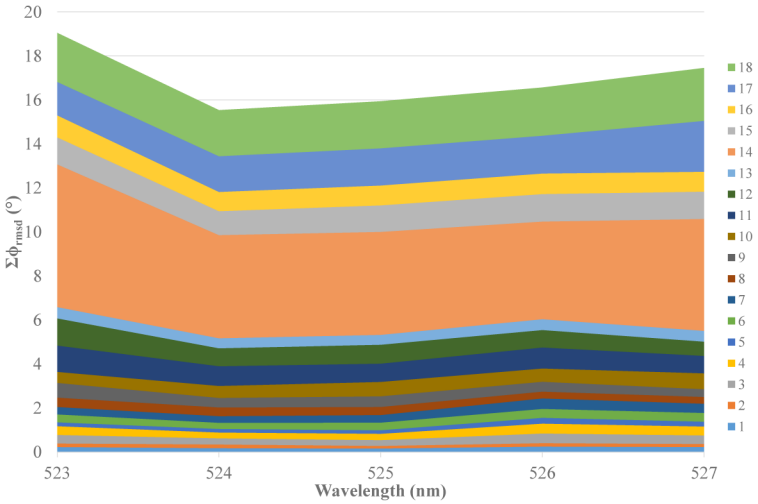

Fig. 6. Evolution of $\Sigma\varphi_{RMSD}$ at 795 nm when depositing the 18 first layers.

The beginning of the strategy for all optical monitoring of the equalizing filter is therefore:

$$[1-18]@524\,nm. \tag{4}$$

To determine the second part of the strategy, we considered again the trinary mapping in Fig. 2 and focused on the analysis of the remaining layers. We analyzed the spectral regions that appear as trigger point monitoring-compatible, starting at layer 19 and plotted for each wavelength, the furthest layers that can be optically monitored with a single wavelength (Fig. 7).

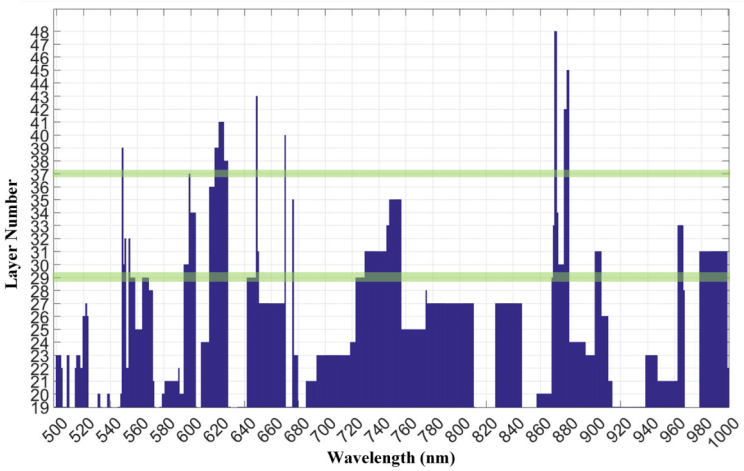

Fig. 7. Maximum number of layers that can be optically monitored with a single wavelength in the [500-1000] nm spectral region starting at layer 19. Layers witnessing a double extremum are colored in green.

One can see that the maximum number of layers that can be optically monitored varies from none to 30, i.e. up to layer 48 or the end of the stack. There are two wavelengths that appear as good candidates for optical monitoring of the remaining stack: 871 and 872 nm. In order to determine if one of these wavelengths appears as the best and if this choice is highly

Optics EXPRESS

critical, we then implemented the PhaseEval method @795 nm when depositing the layers 19 to 48 for monitoring wavelengths between 869 and 874 nm (Fig. 8).

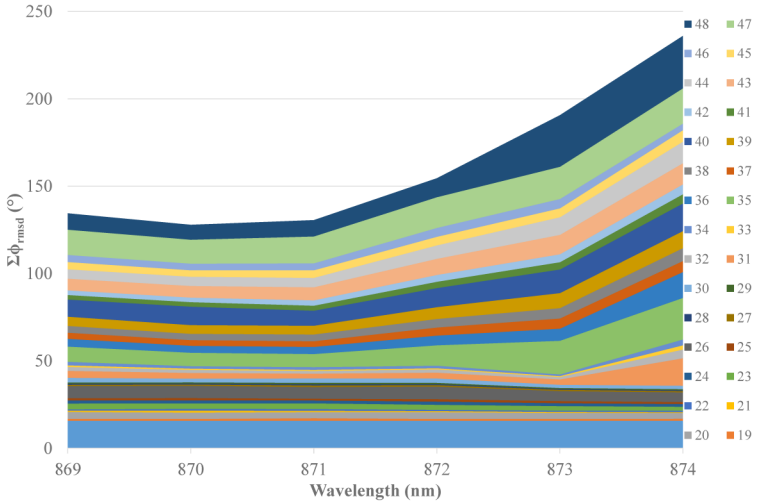

Fig. 8. Evolution of $\Sigma\varphi_{RMSD}$ at 795 nm when depositing the layers 19 to 48 for optical monitoring wavelengths within [869-874] nm spectral range.

One can see that the value of $\Sigma\varphi_{RMSD}$ at achievement varies quite fast with a minimum of 130° at 870 nm and a maximum of 230° at 874 nm (i.e. twice more). In addition, one can see that there are two specific layers that show a small φ_{RMSD} value and therefore a small increase of $\Sigma\varphi_{RMSD}$: layers 29 and 37. This small φ_{RMSD} value for these layers is the result of the phase compensation that occurs when the optical monitoring signal crosses two extrema for the same layer. This result therefore confirms the efficiency of optical monitoring by swing [4] (or Percentage Of Extremum Monitoring (POEM) [5]) to perform phase compensation and the interest to go through these layers during optical monitoring. In addition, Fig. 8 clearly shows that the choice of the right wavelength, with 1 nm precision, is critical to achieve the smallest value of $\Sigma\varphi_{RMSD}$. One can wonder if this difference of a factor 2 of the values of $\Sigma\varphi_{RMSD}$ at 870 and 874 nm are directly transferred into very different discrepancies between theoretical and experimental curves. To illustrate this difference, we simulated, using VDP, the final performances of the filter when monitoring layers 1 to 18 at 524 nm and the layers 19 to 48 with either 870 or 874 nm (Fig. 9).

It is very clear that a large value of $\Sigma\varphi_{RMSD}$ (@795 nm) will result in a poor Figure of Merit. Based on these results, we opted for the wavelength that shows the lowest overall value of $\Sigma\varphi_{RMSD}$, and the lowest φ_{RMSD} of the final layer i.e. 870 nm. The strategy for all optical monitoring of the equalizing filter with two wavelengths is:

$$[1-18]@524\,nm \rightarrow [19-48]@870\,nm. \quad (5)$$

Simulation of the deposition using virtual deposition process (over 100 runs) using the strategy of Eq. (2) results in a Figure of Merit (defined as the average deviation between theoretical and experimental curves) of 1.8%. But one can wonder if better results could be obtained with a different strategy using more wavelengths.

Optics EXPRESS

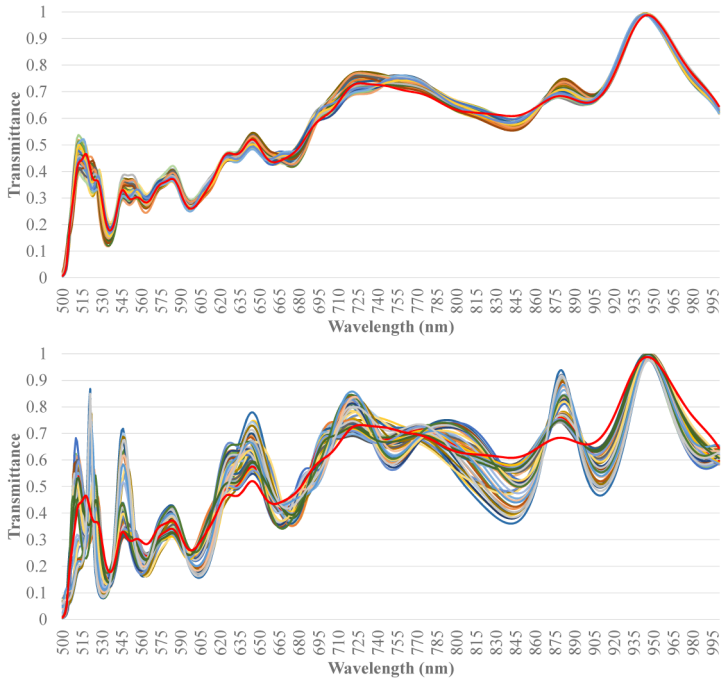

Fig. 9. Simulation of the final spectral performances in the 500-1000 nm range of a filter monitored with [1–18]@524 nm → [19-48]@870 nm (top) and [1–18]@524 nm → [19-48]@874 nm (bottom). The Red curve represents the theoretical result.

3.4.2. Three-wavelength strategy

To determine whether increasing the number of wavelengths allows achieving better filter performances, we analyzed how to generate a new strategy utilizing 3 wavelengths. One can see in Fig. 8 that $\Sigma\varphi_{RMSD}$ stays pretty small for the first 15-20 layers of the second part of the stack and then severely increases for the last ~10 layers with a φ_{RMSD} close to 20° for the layer 47. It would therefore be interesting to change the monitoring wavelength before φ_{RMSD} increases too much.

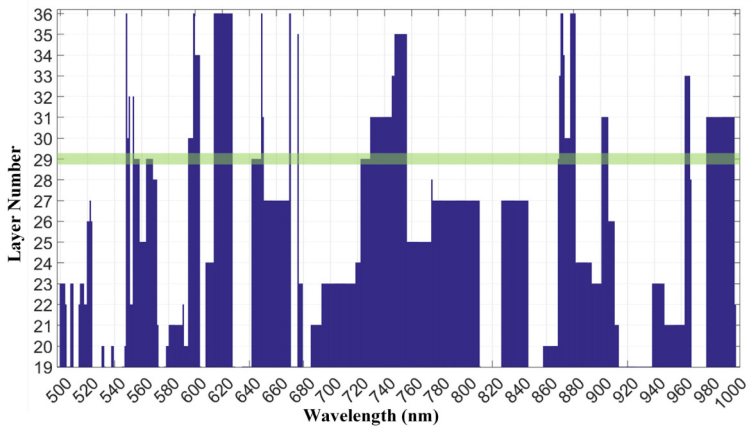

Fig. 10. Maximum number of layers that can be optically monitored with a single wavelength in the [500-1000] nm spectral region starting at layer 19 and ending at layer 36.

Optics EXPRESS

In Fig. 2, layer 37 is associated with a green color, i.e. a thick layer which optical monitoring signal presents two extrema and is therefore optimal for changing the monitoring wavelength. We reanalyzed the Fig. 2 and extracted from it the spectral regions that appear as trigger point monitoring-compatible, starting at layer 19 and up to layer 36 (Fig. 10). One can see that there are 7 distinct regions that allow all-optical monitoring from layer 19 up to layer 36: [548-551] nm, [598-601] nm, three narrow regions in the [603-671] nm range and 2 narrow regions in the [865-885] nm range and associated with the first 2-wavelength strategy. In order to determine which of these wavelengths appears as the best, we then calculated the evolution of $\Sigma\varphi_{RMSD}$ at 795 nm when depositing the layers 19 to 36 for each spectral region (Fig. 11) but the last 2 as the results were already computed in Fig. 8.

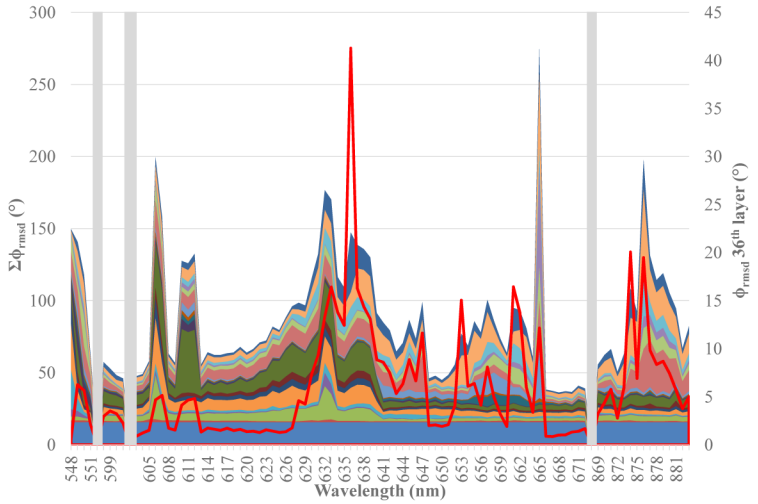

Fig. 11. Evolution of $\Sigma\varphi_{RMSD}$ at 795 nm when depositing the layers 19 to 36 for different range of optical monitoring wavelengths. The red curve represent the φ_{RMSD} at the last layer.

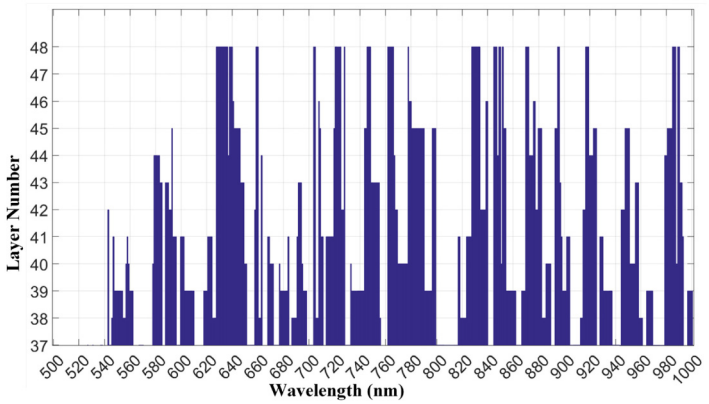

Fig. 12. Maximum number of layers that can be optically monitored with a single wavelength in the [500-1000] nm spectral region starting at layer 37 and up to layer 48.

One can see that the value of $\Sigma\varphi_{RMSD}$ shows some peaks coinciding with grey regions of Fig. 2 and narrow uniform regions with a low value of $\Sigma\varphi_{RMSD}$ (795 nm) at layer 36 with a minimum value within [666-672] nm spectral range. It is therefore legitimate to select a wavelength within this band. There are some fluctuations in this range, but those one are pretty small and might be related to the statistical nature of the analysis. We opted for the

Optics EXPRESS

wavelength that shows the lowest overall value of $\Sigma\varphi_{RMSD}$, and the lowest φ_{RMSD} of the final layer i.e. 670 nm. The strategy for all optical monitoring of the equalizing filter becomes:

$$[1-18]@524\,nm \rightarrow [19-36]@670\,nm. \quad (6)$$

We repeated the same work as above and re-analyzed the Fig. 2 to extract the spectral regions that appear as trigger point monitoring-compatible, starting at layer 37 and up to layer 48 (Fig. 12). One can see that there are 18 distinct regions that allow all-optical monitoring from layer 37 up to layer 48: all between 620 and 1000 nm. In order to determine which of these wavelengths appears as the best, we then calculated the evolution of $\Sigma\varphi_{RMSD}$ @795 nm when depositing the layers 37 to 48 for these spectral regions (Fig. 13).

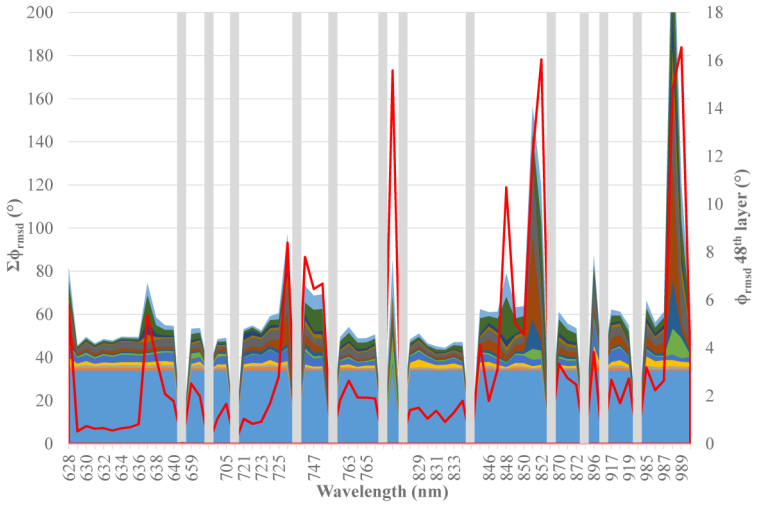

Fig. 13. Evolution of $\Sigma\varphi_{RMSD}$ @795 nm when depositing the layers 37 to 48 in the [620-1000] nm spectral range. The red curve represent the φ_{RMSD} at the last layer.

One can see that the value of $\Sigma\varphi_{RMSD}$ shows some peaks coinciding with grey regions of Fig. 2 and narrow uniform regions with a low value of $\Sigma\varphi_{RMSD}$ (795 nm) at layer 48 with a minimum value within two distinct spectral regions: [629-636] and [828-834] nm. There are some fluctuations in this range, however, the two $\Sigma\varphi_{RMSD}$, values result in pretty much the same at 629 and 832 nm and one value was thus arbitrarily selected. It is interesting also to note that the $\Sigma\varphi_{RMSD}$ @795 nm at layer 48 after depositing layers 19 to 48 with the two-wavelength procedure is ~45°, i.e. more than twice smaller than the one obtained when monitoring layers 19 to 48 with a single wavelength of 870 nm.

The strategy for all optical monitoring of the equalizing filter with three wavelengths is:

$$[1-18]@524\,nm \rightarrow [19-36]@670\,nm \rightarrow [37-48]@832\,nm. \quad (7)$$

We finally simulated the final performances of the filter when depositing over 100 runs using the strategy of Eq. (5) (Fig. 14). A Figure of Merit of 0.87%, i.e. more than 50% better than the one obtained with the two-wavelength strategy is achieved, confirming that a lower value of $\Sigma\varphi_{RMSD}$ results in a better performance in intensity of the filter (similar performances are achieved whether 629 and 832 nm are used as third monitoring wavelength).

Optics EXPRESS

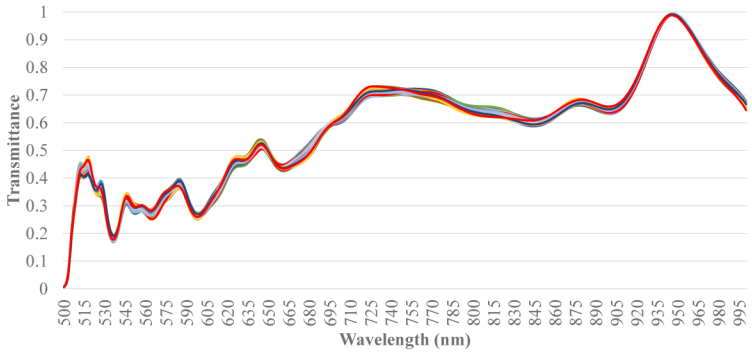

Fig. 14. Simulation of the final spectral performances in the 500-1000 nm range of a filter monitored with [1–18]@524 nm → [19-36]@670 nm → [37-48]@629 nm. The Red curve represents the theoretical result.

The next step is to wonder once more if a better optical monitoring strategy can be achieved if the proposed method is further applied to introduce a fourth monitoring wavelength.

3.4.3. Four-wavelength strategy

While there is no clear evidence of a divergence of the value of $\Sigma\varphi_{RMSD}$ using the three-wavelength optical monitoring strategy, we investigated if using a larger number of monitoring wavelengths allows achieving even better performances. We therefore included a fourth optical monitoring wavelength and decided to cut the monitoring of the layers [19 to 36] into two stacks: layers [19 to 28] and layers [29 to 37] and to use the presence of two extrema in the optical monitoring signal when monitoring layer 29. It is obvious that there are many other possibilities that should be considered. But the goal of this work was to propose a robust technique that allows generating various all-optical monitoring strategies (i.e. all compatible with trigger point monitoring and without quartz-crystal monitored layers) in a semi-automatic way. Let us implement this strategy. To generate this strategy, the same work that was applied in the strategy using 3 wavelengths must be done. For layer 1 to 18, 524 nm is still the optimal monitoring wavelength from a PhaseEval method point of view (Fig. 6). Let us now analyze how to optically monitor the three new selected stacks [19 to 28], [29 to 36] and [37 to 48].

We plotted in Fig. 15 an overlay between $\Sigma\varphi_{RMSD}$ and the spectral regions that appear as trigger point monitoring-compatible based on trinary mapping (non-greyish rectangles), for the layers 19 to 28 versus the optical monitoring wavelength and the same type of information for the stacks [29 to 36] and [37 to 48] respectively in Figs. 16 and 17.

An identical analysis to the one performed in the previous section allows selecting, for each stack, the wavelength that results in the smallest value of $\Sigma\varphi_{RMSD}$ at layer 48 and equal to about 42°. The $\Sigma\varphi_{RMSD}$ value is very close to the one achieved with the 3-wavelength strategy. We can also note that the difference of final φ_{RMSD} between the two strategies is not significant (both around 1°). Finally, the strategy for all optical monitoring of the equalizing filter with four wavelengths is:

$$[1-18]@524\,nm \rightarrow [19-28]@740nm \\ \rightarrow [29-36]@790\,nm \rightarrow [37-48]@629nm. \quad (8)$$

Optics EXPRESS

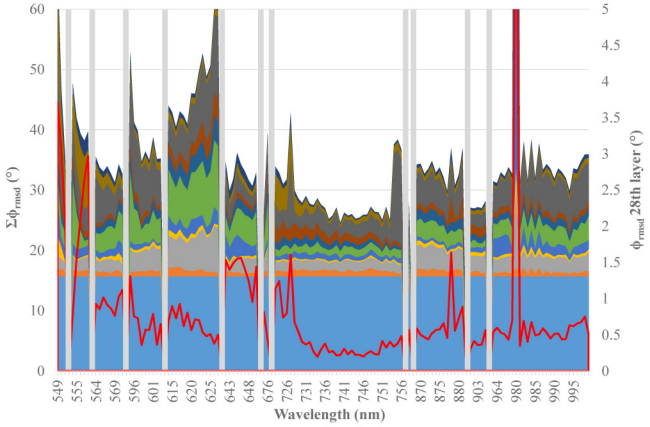

Fig. 15. Evolution of $\Sigma\varphi_{RMSD}$ versus optical monitoring wavelength for the layers 19 to 28 and overlay with the regions that are trigger point monitoring-compatible based on trinary mapping (non-greyish rectangles). The red curve represent the φ_{RMSD} at the last layer.

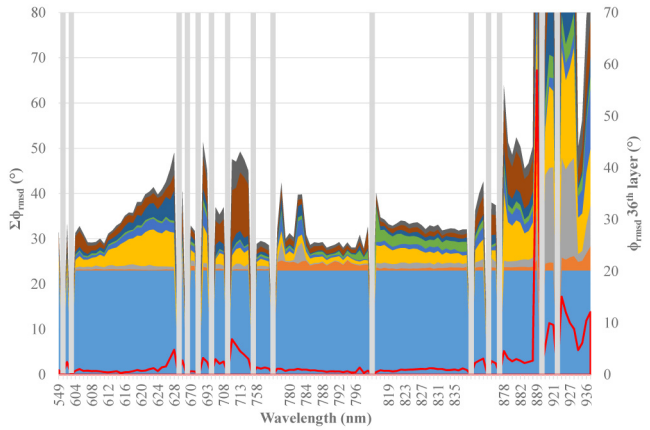

Fig. 16. Evolution of $\Sigma\varphi_{RMSD}$ versus optical monitoring wavelength for the layers 29 to 36 and overlay with the regions that are trigger point monitoring-compatible based on trinary mapping (non-greyish rectangles). The red curve represent the φ_{RMSD} at the last layer.

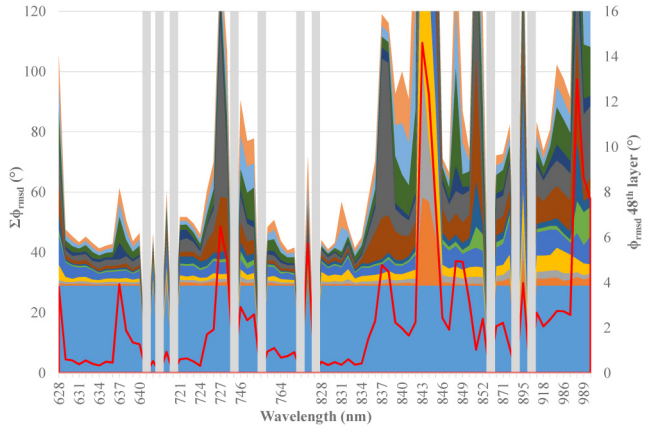

Fig. 17. Evolution of $\Sigma\varphi_{RMSD}$ versus optical monitoring wavelength for the layers 37 to 48 and overlay with the regions that are trigger point monitoring-compatible based on trinary mapping (non-greyish rectangles). The red curve represent the φ_{RMSD} at the last layer.

Optics EXPRESS

We finally simulated the final performances of the filter when depositing over 100 runs using the strategy of Eq. (6) (Fig. 18). The Figure of Merit is 1.37%, i.e. not better than the three-wavelength strategy, confirming that, using the proposed approach, there is no gain in increasing the number of monitoring wavelengths.

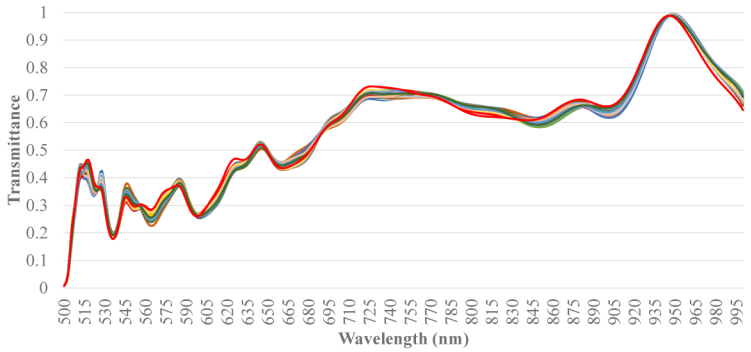

Fig. 18. Simulation of the final spectral performances in the 500-1000 nm range of a filter monitored with [1–18]@524 nm → [19-28]@740 nm→ [29-36]@790 nm → [37-48]@629 nm. The Red curve represents the theoretical result.

4. Experimental demonstration of an equalizing filter

The previous analysis of the determination of an all-optical monitoring procedure is of interest only if it is confirmed by experimental results. To carry out this work, we fabricated a prototype of this filter using a Bühler HELIOS machine combined with an OMS 5000 optical monitoring system. We did not test all the procedures but only the one that provided the best results when simulated using the VDP, i.e. a three-wavelength strategy presented in Eq. (4).

The equalizing filter was deposited on a fused silica substrate. Then, the spectral dependence of the transmission of this filter was measured in the [500-1000] nm spectral range, using a Perkin Elmer Lambda 1050 (Fig. 19).

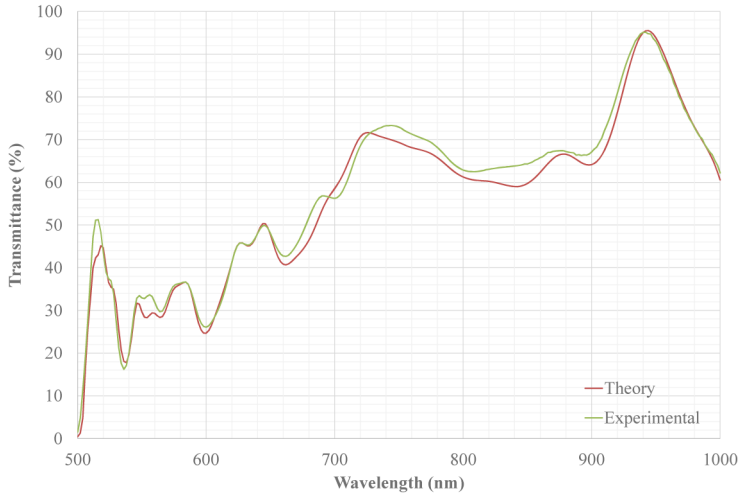

Fig. 19. Experimental spectral performances in the 500-1000 nm range of a filter monitored with [1–18]@524 nm → [19-36]@670 nm → [37-48]@832 nm. The red curve represents the theoretical result and the green one the experimental result.

Using this all-optical monitoring strategy that was generated in a semi-automatic way, we were able to fabricate a complex optical interference filter that presents low deviation between the experimental and the theoretical spectral transmission resulting in a Figure of

Optics EXPRESS

Merit of 2.18%. This Figure of Merit is 2.5 times larger than the one that was predicted by the VDP software. Such a difference can be easily explained by the fact that both the strategy and the VDP simulations were performed with software that were developed internally and that might not perfectly reproduce the procedures and errors of an OMS 5000 system. Improvement of these results would thus be possible by optimizing the VDP software in order to better reproduce the OMS 5000 performances. However, independently from these small discrepancies, one must keep in mind that the final performances of such a filter quickly diverge if not properly monitored, confirming that the proposed all-optical monitoring strategy is efficient and that the errors on the thickness of each layer have been minimized.

5. Conclusion

We have presented a rigorous method for the determination of various optical monitoring strategies of an optical filter that presents 48 layers with an arbitrary thickness distribution. This method relies on the combination of trinary mapping and PhaseEval method. Using this technique, we have presented three different optical monitoring strategies based on 2, 3 and 4 different wavelengths and have shown that all of them allow all-optical monitoring of the whole filter and result in very low discrepancies between the final theoretical and simulated spectral performances of the filter, confirming that the method permits an efficient semi-automatic determination of strategies.

We have opted for some choices that limited the number of possible cases (see Fig. 3), such as this method does not allow to generate the best optical monitoring strategy, but at least an efficient one. Among these choices, the main two criteria were:

- We selected monitoring wavelengths that allow monitoring the largest number of layers with a single one unless specified differently. This was the case when choosing the first monitoring wavelength for all proposed strategies.
- We forced changes of a monitoring wavelength on layers which associated optical monitoring signal presents two extrema in order to fully benefit from POEM phase compensation.

We see that in case of the first layer, it would have been possible to keep the second criterion and change the wavelength before reaching layer 18, for example before layer 14. However, one can see that in that case, we would not have limited the number of possible paths and the number of possible solutions would have become infinite. Many other strategies could have been implemented. However, the proposed work was not intended to provide the best optimal method for determining optical monitoring strategies. It is one example among several other possible ones. This method has proven to be efficient on various examples [10,11] including this complex filter. But most of all, it provides different tools that properly combined, allow determining all-optical monitoring strategies in an automatic or semi-automatic way.

Acknowledgments

This work was performed within the LabTOP (Laboratoire commun de Traitement OPtique des surfaces), a research cooperation agreement between Institut Fresnel (Aix-Marseille Univ, CNRS, Centrale Marseille) and CILAS Company.

References

1. K. D. Hendrix, C. A. Hulse, G. J. Ockenfuss, and R. B. Sargent, “Demonstration of narrowband notch and multi-notch filters,” Proc. SPIE **7067**, 706702 (2008).
2. M. Scherer, J. Pistner, and W. Lehnert, “UV- and VIS filter coatings by plasma assisted reactive magnetron sputtering (PARMS),” in Optical Interference Coatings (Optical Society of America, 2010), paper MA7.
3. T. Begou, H. Krol, D. Stojcevski, F. Lemarchand, M. Lequime, C. Grezes-Besset, and J. Lumeau, “Complex optical interference filters with stress compensation for space applications,” CEAS Space J. **9**(4), 441–449 (2017).
4. H. A. Macleod, *Thin-Film Optical Filters* (CRC/Taylor & Francis, 2010).

Optics EXPRESS

5. R. R. Willey, "Simulation comparisons of monitoring strategies in narrow bandpass filters and antireflection coatings," Appl. Opt. **53**(4), A27–A34 (2014).
6. R. R. Willey, "Design and monitoring of narrow bandpass filters composed of non-quarter-wave thicknesses," Proc. SPIE **7101**, 710119 (2008).
7. T. Begou, F. Lemarchand, and J. Lumeau, "Advanced optical interference filters based on metal and dielectric layers," Opt. Express **24**(18), 20925–20937 (2016).
8. A. Zöller, M. Boos, H. Hagedorn, B. Romanov, "Computer simulation of coating processes with monochromatic monitoring," Proc. SPIE **7101**, 71010G (2008).
9. J. A. Dobrowolski, "Modern computational methods for optical thin film systems," Thin Solid Films **34**(2), 313–321 (1976).
10. M. Vignaux, F. Lemarchand, C. Grezes-Besset, J. Lumeau, and J. Lumeau, "In situ optical monitoring of Fabry-Perot multilayer structures: analysis of current techniques and optimized procedures," Opt. Express **25**(15), 18040–18055 (2017).
11. M. Vignaux, F. Lemarchand, T. Begou, C. Grèzes-Besset, and J. Lumeau, "Trinary mappings: a tool for the determination of potential spectral paths for optical monitoring of optical interference filters," Appl. Opt. **57**(24), 7012–7020 (2018).
12. M. Trubetskov, T. Amotchkina, and A. Tikhonravov, "Automated construction of monochromatic monitoring strategies," Appl. Opt. **54**(8), 1900–1909 (2015).
13. A. V. Tikhonravov and M. K. Trubetskov, "OptiLayer software," http://www.optilayer.com.